A STUDY OF THE INFLUENCE OF WATER-SIDE FOULING ON AIR-TO-WATER HEAT EXCHANGER THERMAL PERFORMANCE

C. F. Bowman

CHUCK BOWMAN ASSOCIATES, INC.
KNOXVILLE TENNESSEE

AIR-TO-WATER HEATEXCHANGER ANALYSIS

This case study uses the design point method from Reference 1 to determine the corrected air-side convection film heat transfer coefficient and illustrates the projection of the heat transfer rate for the heat exchanger at limiting conditions based on measurements collected at test conditions. The use of the design point method eliminates the need for air-side heat transfer correlations specific to the geometry and configuration of the heat exchanger. Additional simplifying assumptions for this case study include the following:

1 the number of tube passes are sufficient such that the heat exchanger may be treated as counter-flow heat exchanger;
2 air pressures at the design point, test conditions, and limiting conditions are constant at 14.7 psia;
3 dry air conditions exist at the design point, test conditions, and limiting conditions such that the analysis does not require consideration of condensation of moisture;
4 corrections for both air-side and water-side heat transfer coefficients for variable fluid properties are insignificant;
5 the air-side flow rate is not measured for the test but, instead, is calculated from the heat transfer calculated from the flow and temperatures measured on the water side and the temperature differences measured on the air side;
6 limiting conditions are the same as design conditions;
7 the effects of changes in fluid properties are insignificant in iterating to determine the heat transfer at limiting conditions.

Step 1: State the "TEMA Design Point" Conditions and Assumptions

1. Air-side flow rate, $m_h = 64{,}708$ [lbm/hr]
2. Tube-side flow rate, $m_c = 40{,}418$ [lbm/hr]
3. Air-side inlet temperature, $T_{h,i} = 90$ [°F]
4. Tube-side inlet temperature, $T_{c,i} = 45$ [°F]
5. Air-side outlet temperature, $T_{h,o} = 61.4$ [°F]
6. Tube-side outlet temperature, $T_{c,o} = 56$ [°F]
7. Heat transfer rate, $Q = 444{,}600$ [Btu/hr]
8. Air-side fouling resistance, $R_{f,h} = 0.0005$ [hr-ft^2-°F/Btu]
9. Tube-side fouling resistance, $R_{f,c} = 0.0005$ [hr-ft^2-°F/Btu]
10. Tube-side thermal conductivity, $k_c = 0.337$ [Btu/(hr-ft-°F)]
11. Air-side thermal conductivity, $k_h = 0.0157$ [Btu/(hr-ft-°F)]
12. Tube-side absolute viscosity, $\mu_c = 3.25$ [lbm/(ft-hr)]
13. Air-side absolute viscosity, $\mu_h = 0.045$ [lbm/(ft-hr)]
14. Tube-side density, $\rho = 62.4$ [lbm/ft^3]
15. Tube-side specific heat, $c_{p,c} = 0.999$ [Btu/(lbm-°F)]
16. Air-side specific heat, $c_{p,h} = 0.24$ [Btu/(lbm-°F)]
17. Total effective area of finned surface, $A_h = 2{,}731.73$ [ft^2]
18. Ratio of finned side to inside area, $A_h/A_c = 22.84$
19. Inside tube diameter, $D_i = 0.0474$ [ft]
20. Inside tube diameter, $d_i = 0.569$ [in]

21. Outside tube diameter, $D_o = 0.0521$ [ft]
22. Outside tube diameter, $d_o = 0.625$ [in]
23. Fin efficiency, $h_{f,h} = 0.72$
24. Tube material thermal conductivity, $k_w = 225$ [Btu/(hr-ft-°F)]
25. Number of tubes carrying flow, $N_t = 30$
26. Number of fins per foot, $N_f = 96$
27. Fin thickness, $\delta = 0.000833$ [ft]
28. Tube wall thickness, $t = 0.028$ [in]
29. Log mean temperature correction factor, $F = 1.0$

Step 2: Define variables

1. Greater terminal temperature difference, $\Delta T_1 = T_{h,i} - T_{c,o}$ [°F]
2. Lesser terminal temperature difference, $\Delta T_2 = T_{h,o} - T_{c,i}$ [°F]
3. Log mean temperature difference, $LMTD = (\Delta T_1 - \Delta T_2)/\ln(\Delta T_1/\Delta T_2)$ [°F]
4. Effective mean temperature difference, $EMTD = F\ (LMTD)$ [°F]
5. Overall heat transfer coefficient, $U = Q/(A_h F\ LMTD)$ [Btu/(hr ft^2 °F)]
   $= 1/\{A/(A_h \eta_h h_h) + (A/A_w) R_w + A/(A_c \eta_c h_c)$
6. Tube wall Resistance, $R_w = (D_o - D_i)/2\ k_w$ [(hr ft^2 °F)/Btu]
7. Inside tube area, $A_c = A_h (A_c/A_h)$ [ft^2]
8. Outside tube area, $A_o = (D_o/D_i)\ A_c$ [ft^2]
9. Tube wall area, $A_w = (A_o - A_i)/\ln A_o/A_I$ [ft^2]
10. Mass flow rate per tube, $m_t = m_o/N_t$ [Lbm/hr]
11. Volumetric flow rate per tube, $V_t = m_t/\rho$ [ft^3/hr]
12. Flow area of tube, $a_t = (\pi/4)\ D_i^2$ [ft^2]
13. Tube velocity, $v_t = V_t / a_t$ [ft/hr]
14. Tube-side Prandtl number, $Pr_c = c_{p,c}\ \mu_c / k_c$
15. Tube-side Reynolds number, $Re_c = \rho\ v_t\ D_i / \mu_c$
16. Fanning friction factor, $f = (1.58 \ln Re_c - 3.28)^{-2}$
17. Nusselt number, $Nu = ((f/2)\ Re_c\ Pr_c)/(1.07 + 12.7(f/2)^{-2}\ (Pr_c^{2/3} - 1))$
18. Tube-side film coefficient, $h_c = Nu\ (k_c / D_i)$ [Btu/(hr ft^2 °F)]
19. Area of the finned side per fin $a_h = (A_o/A_h)\ \pi\ D_i / N_f$
20. Area of the prime per fin, $a_p = \pi\ D_o \{(1/N_f) - \delta\}$
21. Area of the fin per fin, $a_f = a_h - a_p$ [ft^2/fin]
22. Surface efficiency $\eta_h = (a_p + a_f \eta_f)/a_h$
23. Total fouling resistance, $R_f = (R_{f,h}/\eta_h) + (A_h/A_c)\ R_{f,c}$ [(hr ft^2 °F)/Btu]

Step 3: Compute the Overall Heat Transfer Coefficient

$\Delta T_1 = T_{h,i} - T_{c,o} = 34$ [°F]
$\Delta T_2 = T_{h,o} - T_{c,i} = 16.4$ [°F]
$LMTD = (\Delta T_1 - \Delta T_2)/\ln(\Delta T_1/\Delta T_2) = 24.1$ [°F]
$EMTD = F\ (LMTD) = 1\ (LMTD) = 24.1$ [°F]
$U = Q/(A_h\ EMTD) = 6.74$ [Btu/(hr ft^2 °F)]

Step 4: Compute the Resistances to Heat Transfer at "Design Point" Conditions

First, compute the tube wall resistance and associated areas.

$R_w = (D_o - D_i)/2\ k_w = 0.00001$ [(hr ft^2 °F)/Btu]
$A_c = A_h\ (A_c/A_h) = 119.6$ [ft^2]
$A_o = (D_o/D_i)\ A_c = 131.4$ [ft^2]
$A_w = (A_o - A_i)/\ln A_o/A_i = 125.4$ [ft^2]

Next compute the tube-side film coefficient at "Design Point" conditions.

$m_t = m_c/N_t = 1347.27$ [Lbm/hr]
$V_t = m_t / \rho = 21.59$ [ft^3/hr]
$a_t = (\pi/4)\, D_i^2 = 0.00177$ [ft^2]
$v_t = V_t / a_t = 12{,}227$ [ft/hr]
$Pr_c = c_{p,c}\, \mu_c / k_c = 9.6$
$Re_c = \rho\, v_t\, D_i / \mu_c = 11{,}100$
$f = (1.58 \ln Re_c - 3.28)^{-2} = 0.00764$
$Nu = ((f/2)\, Re_c\, Pr_c)/(1.07+12.7(f/2)^{1/2}\,(Pr_c^{2/3}-1)) = 106.63$
$h_c = Nu\,(k_c / D_i) = 758$ [Btu/(hr ft^2 °F)]

Then compute the air-side surface efficiency, η_h, from the area ratios and the fin efficiency.

$a_h = (A_h/A_c)\, \pi\, D_i / N_f = 0.03544$ [ft^2/fin]
$a_p = \pi\, D_o\, \{(1/N_f) - \delta\} = 0.00157$ [ft^2/fin]
$a_f = a_h - a_p = 0.03387$ [ft^2/fin]
$\eta_h = (a_p + a_f \eta_f)/a_h = 0.732$

The air-side and tube-side fouling resistances, $R_{f,h}$ and $R_{f,c}$, are both given as 0.0005 (hr-ft^2-°F)/Btu
Therefore, the total fouling resistance is,

$$R_f = (R_{f,h} / \eta_h) + (A_h/A_c)\, R_{f,c} = 0.0121 \ [(\text{hr ft}^2\ °\text{F})/\text{Btu}]$$

Step 5: Compute the air-side film coefficient at "Design Point" Conditions

Since,

$$1/U = A/(A_h\, \eta_h\, h_h) + (A/A_w)\, R_w + A/(A_c\, \eta_c\, h_c) + R_f$$

where h_h and h_c are the hot and cold side coefficients of heat transfer. If one takes the hot side area
the reference area,

$$A = A_h$$

and since

$$\eta_c = 1,$$

then,

$$1/U = 1/(\eta_h\, h_h) + (A_h/A_w)\, R_w + A_h/(A_c\, h_c) + R_f$$

And

$$h_h = 1/(\eta_h) / \{1/U - R_f - (A_h/A_w)\, R_w - A_h/(A_c\, h_c)\} = 13.1 \ [\text{Btu/(hr ft}^2\ °\text{F})]$$

Step 6: Compute the Tube-side Fouling at Test Conditions

Test results are as follows:

$m_c = 43{,}000$ lbm/hr
$T_{h,i} = 90.0$ °F
$T_{c,i} = 46.0$ °F
$T_{h,o} = 65.0$ °F
$T_{c,o} = 57.0$ °F

From these results, the following values may be determined:

$k_c = 0.337$ [Btu/(hr-ft-°F)]
$k_h = 0.0157$ [Btu/(hr-ft-°F)]
$\mu_c = 3.25$ [lbm/(ft-hr)]
$\mu_a = 0.045$ [lbm/(ft-hr)]
$\rho = 62.4$ [lbm/ft^3]
$c_{p,c} = 0.999$ [Btu/(lbm-°F)]
$c_{p,h} = 0.24$ [Btu/(lbm-°F)]
$\Delta T_1 = T_{h,i} - T_{c,o} = 33.0$ [°F]
$\Delta T_2 = T_{h,o} - T_{c,i} = 19.0$ [°F]
$LMTD = (\Delta T_1 - \Delta T_2)/\ln(\Delta T_1/\Delta T_2) = 25.4$ [°F]
$F = 1.0$
$EMTD = F\,(LMTD) = 25.4$ [°F]
$Q = m_c\, c_{p,c}\, (T_{c,o} - T_{c,i}) = 472{,}527$ [Btu/hr]
$U = Q/(A_h\, EMTD) = 6.82$ [Btu/(hr ft^2 °F)]
$m_t = m_c/N_t = 1{,}433.33$ [Lbm/hr]
$V_t = m_t / \rho = 22.97$ [ft^3/hr]
$a_t = (\pi/4)\, D_i^2 = 0.00177$ [ft^2]
$v_t = V_t / a_t = 13{,}008$ [ft/hr]
$Pr_c = c_{p,c}\, \mu_c / k_c = 9.6$
$Re_c = \rho\, v_t\, D_i / \mu_c = 11{,}800$
$f = (1.58 \ln Re_c - 3.28)^{-2} = 0.00751$
$Nu = ((f/2)\, Re_c\, Pr_c)/(1.07 + 12.7(f/2)^{1/2}\,(Pr_c^{2/3} - 1)) = 112.21$
$h_c = Nu\,(k_c / D_i) = 797$ [Btu/(hr ft^2 °F)]

One must calculate a new value for h_h based on the test conditions on the air side, since Re and Pr for the air side will be different than was the case for the "Design Point" conditions. However, one is not required to calculate the absolute values of Re and Pr on the air side. Assuming conservation of energy, one may calculate the air-side mass flow rate under test conditions as follows:

$$m_h = m_c \left(\frac{c_{p,c}}{c_{p,h}}\right)\left(\frac{T_{c,o} - T_{c,i}}{T_{h,o} - T_{h,i}}\right) = 78{,}755\,[Lbm/hr]$$

Then the value for h_h based on the test conditions on the air side may be computed based on a correlation by Taborek (Reference 2). If one assumes that the actual value for h_h is a function of some ideal value for the air-side thermal conductivity for pure cross flow such that

$$h_h = J_T\; h_{h,ideal}$$

where J_T is a correction factor that is a function of the various leakage and bypass paths and, therefore, remain constant for a given heat exchanger. Therefore,

$$J_T = \left(\frac{h_h}{h_{h,ideal}}\right)_{design} = \left(\frac{h_h}{h_{h,ideal}}\right)_{test}$$

and

$$(h_h)_{test} = \left(\frac{h_{h,test}}{h_{h,design}}\right)_{ideal}\; h_{h,design}$$

From the Taborek correlation,

$$h_h = 0.2\,\mathrm{Re}^{0.6}\,\mathrm{Pr}^{.333}\,(\frac{k}{D})$$

substituting,

$$(h_h)_{test} = \frac{[(m_h/\mu_h)^{0.6}\,(\mu_h\,c_{p,h}/k_h)^{1/3}\,k_h]_{test}}{[(m_h/\mu_h)^{0.6}\,(\mu_h\,c_{p,h}/k_h)^{1/3}\,k_h]_{design}}\,h_{h,design} = 14.8\,[Btu/hr-ft^2-{}^oF]$$

Therefore, the total apparent fouling resistance as determined by the test may be computed as,

$$R_f = 1/U - 1/(\eta_h h_h) - (A_h/A_w)\,R_w - A_h/(A_c h_c) = 0.02525\ [(\mathrm{hr\ ft^2\ {}^oF})/\mathrm{Btu}].$$

By assuming that the air-side fouling is constant, at 0.0005 [(hr ft^2 °F)/Btu] one may imply a tube-side fouling resistance.

$$R_{f,c} = (A_o/A_h)\,(R_f - R_{f,h}/\eta_h) = 0.00108\ [(\mathrm{hr\ ft^2\ {}^oF})/\mathrm{Btu}]$$

One should note that this value represents an apparent fouling which also reflects any other deficiencies in the heat exchanger and may be very misleading.

Step 7: Compute the Heat Transfer at Limiting Conditions

In this example, the limiting conditions are the same as the design point conditions. Therefore, the values for fluid properties are the same as those for the design point.

Lestina and Scott (Reference 3) showed that the heat transfer at limiting conditions, Q*, is a function of the heat transfer at test conditions, and one is not required to calculate the fouling. The following are the three correction terms (assuming that the change in fin efficiency and tube material thermal conductivity are negligible):

$$E' = \frac{EMTD^*}{EMTD}$$

$$h_h' = \frac{1}{\eta_h}(\frac{1}{h_h^*} - \frac{1}{h_h})$$

$$h_c' = \frac{1}{h_c^*} - \frac{1}{h_c}$$

So that the heat transfer at limiting conditions, Q*, is

$$Q^* = \frac{Q\,E'}{1 + \left(\frac{Q}{EMTD}\right)\left(\frac{h_h'}{A_h} + \frac{h_c'}{A_c}\right)}$$

If the limiting condition is other than the "Design Point", then the physical properties and flow rates must be used to calculate the appropriate values for Re, Pr, h_i and h_o for that particular condition.

The final solution is iterative because outlet temperatures and the EMTD are a function of Q*. Therefore, by iteration the heat transfer at limiting conditions is

$Q^* = 413{,}000$ [Btu/hr]

INFLUENCE OF WATER-SIDE FOULING ON HEAT TRANSFER

One may calculate the amount of heat transfer that would occur under test conditions from

$Q = U\,A\,EMTD$

where,

$$U = \frac{1}{\frac{1}{\eta_h h_h} + \frac{R_{f,h}}{\eta_h} + \left(\frac{A_h}{A_w}\right)R_w + \left(\frac{A_h}{A_c}\right)R_{f,c} + \left(\frac{A_h}{A_c}\right)\left(\frac{1}{h_c}\right)}$$

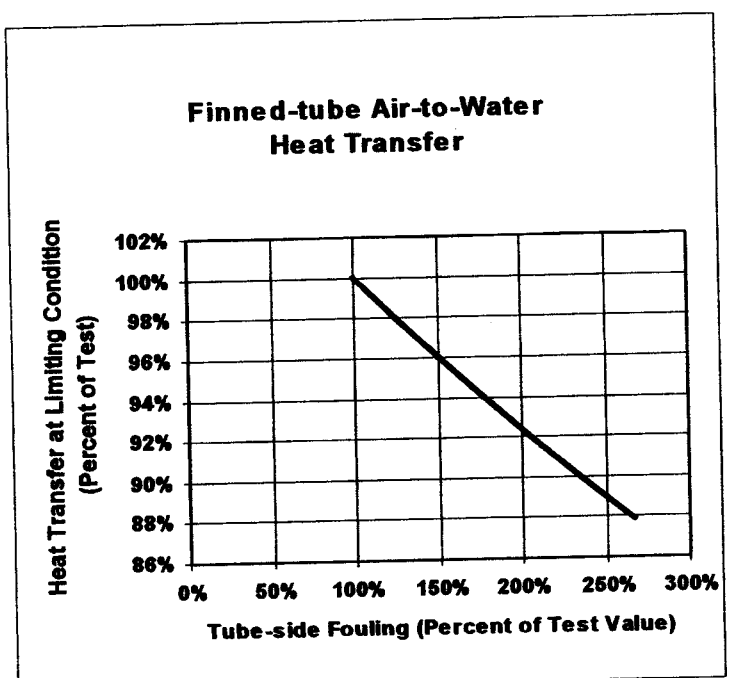

Since all of these terms are known, the water-side fouling may be arbitrarily increased to determine the effect of fouling on heat transfer. The results are shown in Figure 1. This figure illustrates the fact that the tube-side fouling can increase by a factor of three and only reduce the heat transfer rate at limiting conditions by fourteen percent.

The reason for the weak correlation between tube-side fouling and the heat transfer rate is best illustrated by Figure 2. The total resistance to heat transfer for an air-to-water heat exchanger is dominated by the air-side convection boundary resistance. Although the water-side fouling resistance is the second largest contributor to the total resistance, it is normally a small part of the total resistance.

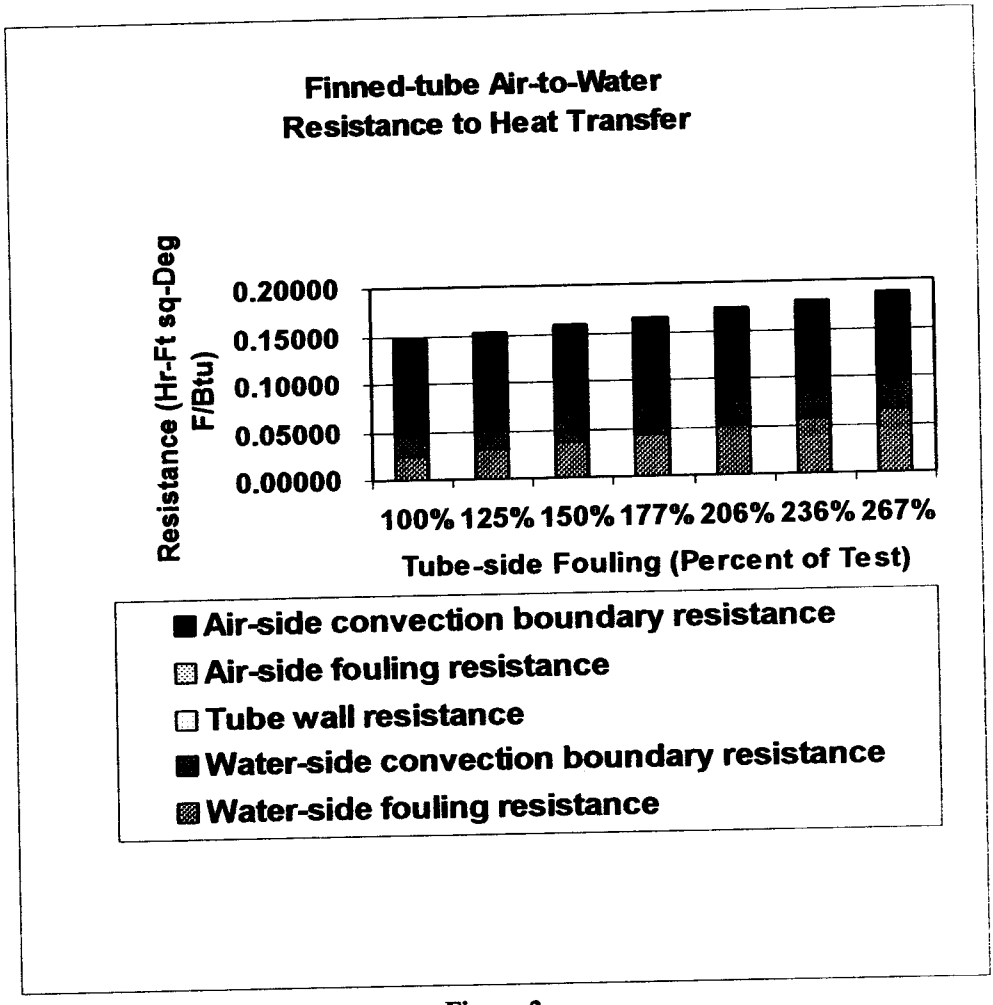

Figure 2

CHARACTERISTICS OF BIOLOGICAL FOULING IN SERVICE WATER SYSTEMS

Taborek (Reference 4) noted that the tube-side fouling rate may be a function of tube-side velocity, tube surface temperature, tube material, and cooling water quality. In some cases, "asymptotic fouling" may occur in which the deposition rate decreases and reaches an equilibrium between deposition and removal due to increased shear forces as the velocity increases. Taborek illustrated this effect as shown in Figure

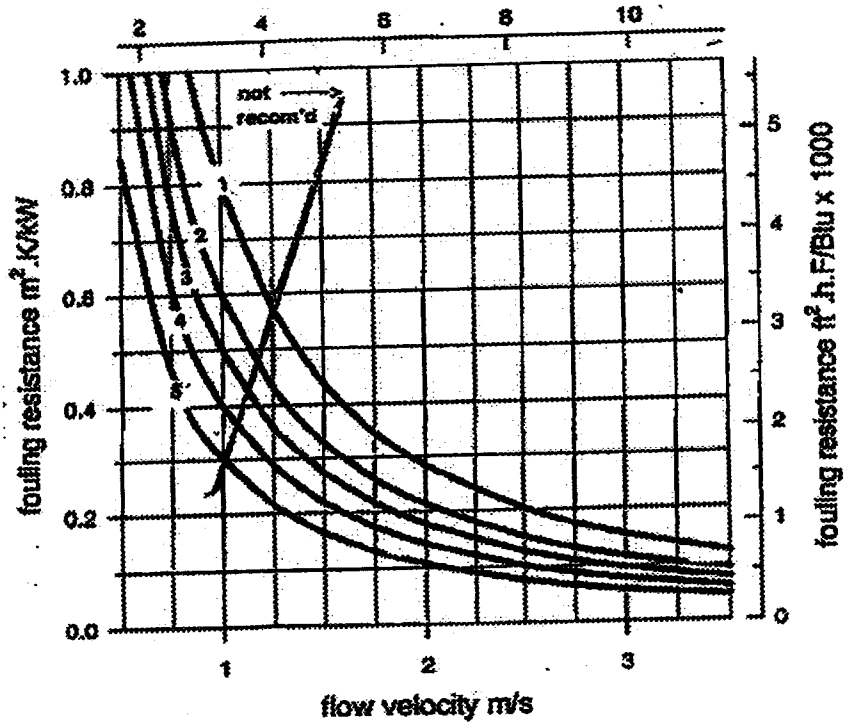

Figure 3

Zelver, et al., (Reference 5) conducted an investigation to determine the rate of fouling in replacement heat exchanger tubing in the containment fan cooler units for a 1000 megawatt nuclear pressurized water reactor. Although the paper did not identify the plant, it would appear to be Indian Point on the Hudson River. The original tubing material was 90-10 copper-nickel and the replacement material was AL-6X. The service water was brackish with variable salinity as a function of tidal changes. This study investigated not only the differences in tubing material but also the impact of flow velocity and tube wall surface temperature on water-side fouling. The rate of fouling was determined by both heat transfer testing and by analysis of the deposit composition. The deposits were found to consist of inorganic silt debris within a matrix of organic material which was approximately 13 percent of the total deposit mass. Figure 4 shows the results of a 140-day test on AL-6X tubing. With a tube velocity of 1.7 ft/sec, heat transfer resistance was observed to increase. On day 82, an immediate and dramatic drop in fouling was observed when the flow velocity was increased to 5.5 [ft/sec] for a one hour period. This flow excursion simulated quarterly testing of the LOCA mode of operation of the system. The effect of flow velocity on fouling was attributed to shear stress at the surface. From Figure 4, one may speculate as to the onset of "asymptotic fouling" just prior to the flow excursion, as the heat transfer resistance seemed to have leveled off. A similar test was conducted on AL-6X tubing without the velocity excursion and on copper-nickel tubing with the velocity excursion. These results shown in Figures 5 and 6 show a similar reduction in the heat transfer resistance for the copper-nickel tubing following the flow excursion. From Figure 5, one may also speculate that there was an onset of "asymptotic fouling" just prior to the flow excursion for the copper-nickel tubing. Although not specifically reported by Zelver, et al., the data in Reference 5 suggests that equilibrium fouling conditions were achieved after approximately 80 days of operation. The study concluded that the tube material influences the fouling rate with the AL-6X being more prone to foul.

Identical tubes were operated at 1.0 and 1.7 [ft/sec] and were monitored for fouling. The study conclude that the lower velocity tubes fouled to a greater extent as would be expected.

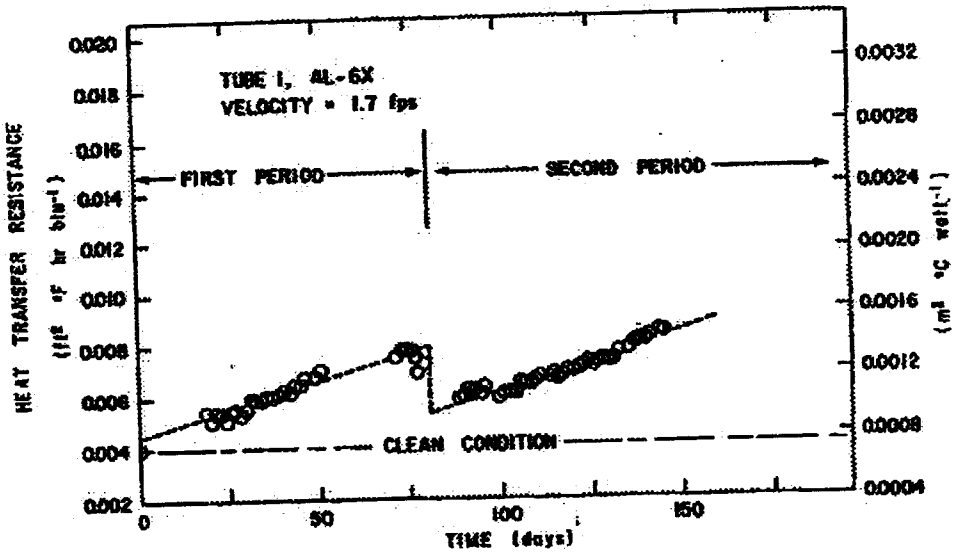

Figure 4

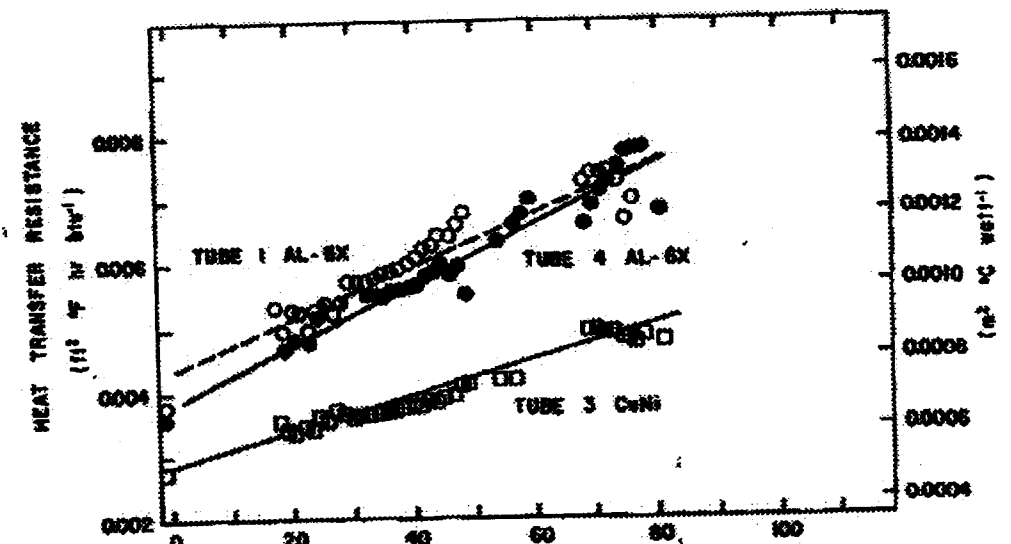

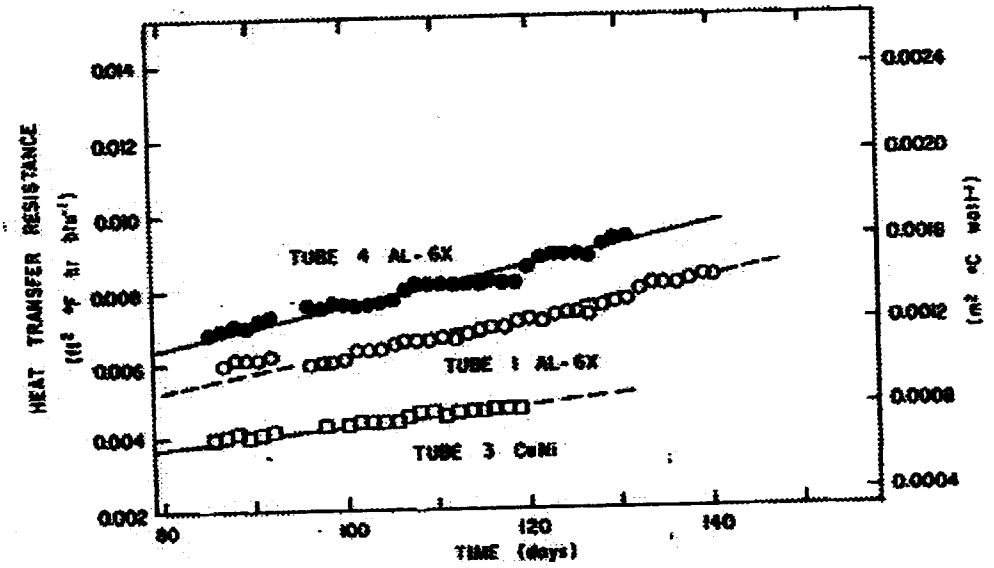

Figure 6

The study also concluded that the tube wall temperature significantly affects fouling, noting that emp
a side-stream monitor to monitor for fouling with unheated tube sections may lead to inaccurate resu

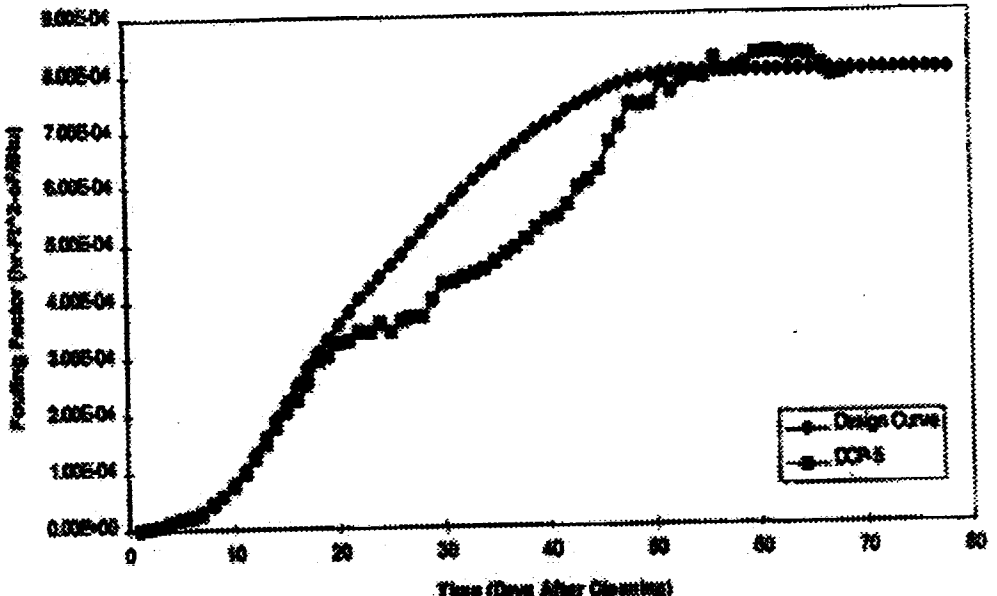

Nolan and Scott (Reference 6) conducted extensive side-stream monitoring tests in response to Generic Letter 89-13. These tests were conducted to study the fouling occurring in the safety-related service water heat exchanger at the Calvert Cliffs Nuclear Power Plant. The results of the tests were to be used to optimize heat exchanger mechanical cleaning and chemical treatment. The service water is brackish water taken from the Chesapeake Bay. Analysis of the fouling deposit composition indicated a biofilm that is a combination of organic activity and inorganic deposits. The organic activity made up approximately 15 percent of the bio-film. The side-stream monitor was designed to model the service water heat exchanger with a tube velocity of 5.54 [ft/sec] and a constant 5 °F rise across the heat exchanger. Figures 7 and 8 show the results of a test conducted in the winter and summer while the cooling water temperature was less than and greater than 55 °F, respectively. The study concluded that the winter equilibrium fouling was approximately 80% of the value measured during the summer. Note that Reference 6 reports fouling resistance, not total heat transfer resistance as in Reference 5. Nolan and Scott distinguished fouling resistance from the other forms of heat transfer resistance using the Wilson method.

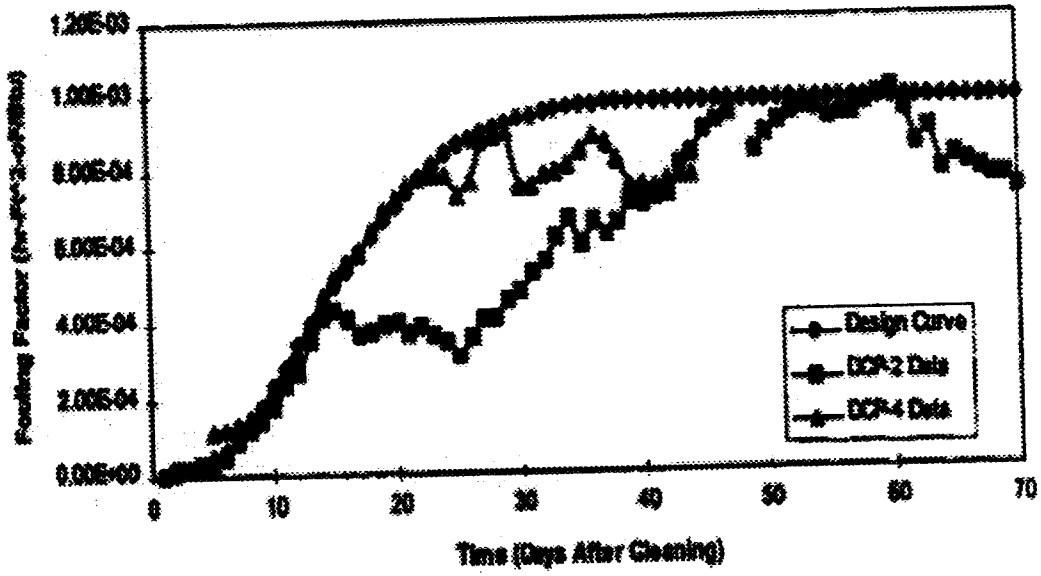

Figure 8

These tests demonstrated that the fouling layer achieves a maximum equilibrium value that is relatively constant and repeatable for a given tube velocity and temperature range. The flow velocity was increased and decreased by approximately 25 percent to determine the impact of of changing shear forces on the equilibrium fouling. The test data showed that the fouling decreased with increased fluid shear force and increased with reduced shear force as would be expected. During summer conditions, the fouling layer reached maximum equilibrium conditions within 30 days after mechanical cleaning. The winter fouling growth rates were approximately 50 % of those measured during the summer. For the particular conditions of these tests, once the bio-film reached a fouling resistance of 0.0004 [hr-ft^2-°F/Btu], it began to interact with the flow stream. The maximum equilibrium fouling was 0.001 [hr-ft^2-°F/Btu] during the summer months. This buildup of tube-side fouling was observed to be repeatable.

Figure 9 shows the fouling reported in References 5 and 6 and the range of fouling resistances recommended by the Tubular Exchangers Manufacturer's Association for river water.

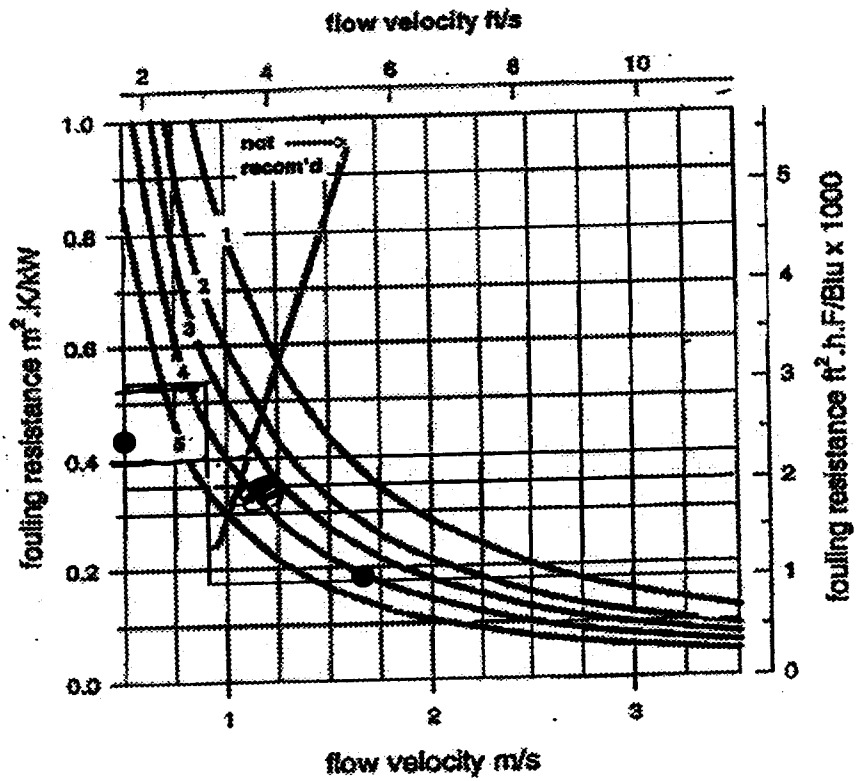

Figure 9

ALTERNATIVES TO THERMAL PERFORMANCE TESTING

Generic Letter 89-13 calls for licensees to conduct a test program to verify the heat transfer capability of all safety-related heat exchangers cooled by service water. Reference 1 provides a menu of alternative methods to satisfy this requirement including not only performance monitoring and heat transfer testing but also temperature monitoring, heat exchanger effectiveness monitoring, pressure drop monitoring and periodic maintenance. Hosterman (Reference 7) suggested that typical heat load calculations used to size heat exchangers for nuclear power plants contain excess conservatism that may be removed to provide additional operating margin. This approach may also be taken to increase the available tube-side fouling resistance. Additionally, the available service water flow to selected heat exchangers may be increased to also increase the available tube-side fouling resistance. If the design basis for the air-to-water heat exchanger may include a conservative estimate of "asymptotic fouling" considering tube-side velocity, surface temperature, tube material, and cooling water quality, the licensee may be able to provide a defensible technical basis for not conducting thermal performance test of these heat exchangers. As a minimum, the following additional steps should be taken on a periodic basis:

1. demonstrate by test that the required cooling water flow rate can be provided for all design basis conditions;
2. demonstrate by pressure drop test that tubes are not plugged on the cooling water side;

3. demonstrate by inspection that the air-side flow paths are unobstructed and the air-side surface is clean.

CONCLUSIONS

Only a weak correlation exists between tube-side fouling and heat transfer in air-to-water heat exchangers. Since the publication of Generic Letter 89-13, a considerable amount of research has been conducted on the characteristics of tube-side raw water fouling in service water systems. In general, the effects of factors such as tube material, tube velocity and tube wall temperature and water quality are known but have not been quantified for specific applications. The combined effects of these factors may be determined and a composite "asymptotic fouling" factor determined that represents the worst case heat exchanger performance for all design basis conditions. The air-to-water heat exchanger could be reanalyzed, reducing overly conservative assumptions and employing the appropriate fouling resistance to conservatively predict heat exchanger performance under limiting conditions. Such an analysis in conjunction with periodic flow and pressure drop testing and regular cleaning and inspections on the air side should satisfy the requirements of Generic Letter 89-13 and make periodic thermal performance testing of air-to-water heat exchangers unnecessary.

REFERENCES

1. Stambaugh, N. and W. Closser, Jr., Heat Exchanger Performance Monitoring Guidelines, EPRI Report NP-7552, Electric Power Research Institute, Palo Alto, CA, 1991
2. Thomas, L. C., Heat Transfer- Professional Version, p. 739, Prentice Hall, Englewood Cliffs, N.
3. Lestina, T. and Scott, B., "Assessing the Uncertainty of Thermal Performance Measurements of Industrial Heat Exchangers", Engineering Foundation Conference of Compact Heat Exchangers for the Process Industries, June 1997.
4. Taborek, J, Assessment of Fouling Research on the Design of Heat Exchangers, Fouling Mitigation of Industrial Heat Exchangers Conference, Shell Beach, CA, 1995.
5. Zelver, N. and W. G. Characklis, J.A. Robinson, F.L. Roe, Z. Dicic, K. Chapple, A. Ribaudo, "Tube Material, Fluid Velocity, Surface Temperature and Fouling: A Field Study", CTI Paper TP 84-16, Cooling Tower Institute, Houston Texas, 1984.
6. Nolan, C.M., and B.H. Scott, "On Line Monitoring of Heat Exchanger Microfouling: An Alternative to Thermal Performance Testing" EPRI Service Water Reliability Improvement Seminar, Electric Power Research Institute, Palo Alto, CA, 1995.
7. Hosterman, E.W., "Reclaiming Heat Exchanger Design Margin An Analytical Approach", EPRI Service Water Reliability Improvement Seminar, Electric Power Research Institute, Palo Alto, CA, 1994